Prevention of amyloid fibril formation of amyloidogenic chicken cystatin by site-specific glycosylation in yeast

JIANWEI HE,[1] YOUTAO SONG,[2] NOBUHIRO UEYAMA,[1] AKIRA SAITO,[3] HIROYUKI AZAKAMI,[1] AND AKIO KATO[1]

[1]Department of Biological Chemistry, Yamaguchi University, Yamaguchi 753-8515, Japan
[2]Department of Life Science, Liaoning Universtity, Shenyang, 110036, China
[3]Institute of Cellular and Molecular Medicine, University of California, San Diego, California 92093, USA

(RECEIVED August 7, 2005; FINAL REVISION October 10, 2005; ACCEPTED October 27, 2005)

Abstract

To address the role of glycosylation on fibrillogenicity of amyloidogenic chicken cystatin, the consensus sequence for *N*-linked glycosylation (Asn_{106}-$Ile_{108} \rightarrow Asn_{106}$-$Thr_{108}$) was introduced by site-directed mutagenesis into the wild-type and amyloidogenic chicken cystatins to construct the glycosylated form of chicken cystatins. Both the glycosylated and unglycosylated forms of wild-type and amyloidogenic mutant I66Q cystatin were expressed and secreted in a culture medium of yeast *Pichia pastoris* transformants. Comparison of the amount of insoluble aggregate, the secondary structure, and fibrillogenicity has shown that the *N*-linked glycosylation could prevent amyloid fibril formation of amyloidogenic chicken cystatin secreted in yeast cells without affecting its inhibitory activities. Further study showed this glycosylation could inhibit the formation of cystatin dimers. Therefore, our data strongly suggested that the mechanism causing the prevention of amyloidogenic cystation fibril formation may be realized through suppression of the formation of three-dimensional domain-swapped dimers and oligomers of amyloidogenic cystatin by the glycosylated chains at position 106.

Keywords: amyloidogenic chicken cystatin; amyloid fibrils; *Pichia pastoris*; glycosylation modification; quality control

Human cystatin C amyloid angiopathy (HCCAA) is a dominantly inherited disorder characterized by tissue deposition of amyloid fibrils in blood vessels that leads to recurrent hemorrhagic stroke (Sanders et al. 2004). It was suggested that a point mutation responsible for the amino acid substitution, a glutamine residue replacing a leucine residue at position 68 in the cystatin C polypeptide chain, could constitute the genetic background to HCCAA disease (Abrahamson 1996). The L68Q variant can form highly stable and domain-swapped dimers at physiological protein concentrations, thus forming part of the amyloidogenic deposits in the brain arteries of young adults, which leads to fatal cerebral hemorrhage (Olafsson and Grubb 2000). The disease also results in paralysis, a development of dementia due to multiple strokes, and death from cerebral hemorrhage before 40 years of age (Abrahamson and Grubb 1994).

The three-dimensional structure of human cystatin C (hcC) is similar to that described for the homologous protein chicken cystatin (cC), and this has been confirmed by NMR studies (Turk et al. 1983; Schwabe et

Reprint requests to: Akio Kato, Department of Biological Chemistry, Yamaguchi University, Yamaguchi 753-8515, Japan; e-mail: akiokato@yamaguchi-u.ac.jp; fax: +81-83-933-5820.

Abbreviations: HCCAA, human cystatin C amyloid angiopathy; hcC, human cystatin C; cC, chicken cystatin; CD, circular dichroism; ER, endoplasmic reticulum; PAGE, polyacrylamide gel electrophoresis; RT-PCR, reverse transcriptase-polymerase chain reaction.

Article and publication are at http://www.proteinscience.org/cgi/doi/10.1110/ps.051753306.

al. 1984; Bode et al. 1988; Dieckmann et al. 1993; Ekiel et al. 1997). Structurally, chicken cystatin and human cystatin C share 62.5% similarity (Jaskolski 2001). Each cystatin consists of a five-stranded anti-parallel β-sheet wrapped around a central helix, and both of them have two disulfide bonds and an ~20 residue insertion of an irregular structure between strands 3 and 4. Residue 66 in cC, corresponding to residue 68 in hcC, lies buried in the hydrophobic core of the protein molecule. The amino acid substitution in L68Q variant hcC, where a strongly apolar aliphatic residue is replaced with a polar residue with an amide group in its side chain, would be expected to cause altered intrinsic properties leading to amyloidosis (Olafsson and Grubb 2000; Staniforth et al. 2001). It seems likely that this fact is an exciting finding for understanding the mechanism of human cystatin C amyloid angiopathy. This also provides a possibility to suppress the formation of amyloid fibrils and to improve the solubility of amyloidogenic cystatin.

Both hcC and cC are nonglycosylated proteins. It had been reported that the anti-rotavirus activity of hcC was substantially enhanced by site-directed glycosylation using the yeast expression system (Nakamura et al. 2004). Likewise, *N*-glycosylation at Asn106 greatly improved the freezing stability of recombinant cC over-expressed in yeast *Pichia. pastoris*. In addition to freeze–thawing stability, the thermal and pH stabilities as well as the susceptibility of glycocystatin were also enhanced. Furthermore, the inhibitory activity remained in glycocystatin for the most part compared to that of the unglycosylation form which did not (Jiang et al. 2002; Tzeng and Jiang 2004).

Our previous report had shown that the glycosylated chains could mask the β-strand of amyloidogenic lysozymes from the intermolecular cross-β-sheet association, thus improving the solubility of amyloidogenic lysozymes and suppressing the formation of amyloid fibrils (Song et al. 2001). Nevertheless, cystatin was the first amyloidogenic protein to be shown to oligomerize in a stable form through a 3D domain swapping mechanism that is different from those for amyloidosis of lysozyme and other amyloidogenic proteins. Recently, Bosques and Imperiali (2003) compared the structure, aggregation kinetics, and fibril formation capabilities of glycosylated and unglycosylated peptides derived from the human prion protein (PrP). They found that *N*-linked glycan (at Asn-181) significantly reduced the rate of fibrillization. Furthermore, Libonati and coworkers (Gotte et al. 2003) also demonstrated that glycosylation of ribonuclease B can affect the formation of three-dimensional domain-swapped oligomers. Amyloidogenic proteins, like cystatin, prion proteins, and ribonuclease, have been shown to form dimers by 3D domain swapping (Janowski et al. 2001; Staniforth et al. 2001; Lee and Eisenberg 2003). Thus, it seems possible that inhibition of the domain-swapping process by glycosylation should also suppress the dimerization, polymerization, and fibrillogenesis of amyloidogenic cystatins.

In our previous study, the wild-type and amyloidogenic cC were both secreted in yeast *P. pastoris*. The amyloidogenic mutant I66Q, but not wild-type cystatin, forms insoluble aggregates during cultivation. Moreover, the dimeric and higher aggregate forms of the mutant lost inhibitory potency. During storage of amyloidogenic cC I66Q under physiological and acidic conditions, typical binding capacity with Congo red and Thioflavin T, and the formation of amyloid fibrils were observed, whereas the characteristic of similar amyloidosis was hardly detected for the wild-type recombinant cystatin (He et al. 2005a). Consequently, these experimental results provided us with a good system for investigating the effects of glycosylation on protein amyloidogensis through a 3D domain-swapping mechanism.

The objective of this work has been to produce glycosylated forms of both wild-type and amyloidogenic cC with carbohydrate chains at positions selected to prevent fibril formation. Considering the 3D structure of cC, it seems reasonable that a carbohydrate chain attached closely to the hydrophobic core of cystatin should affect the domain swapping or the hydrogen bond formed by two cystatin-fold units.

Results

N-*Glycosylated and nonglycosylated forms of recombinant mutant cC I108T and I66Q/I108T were both secreted in the broth of* P. pastoris

After 3 days of cultivation when the secreted amounts were maximal, the secretion of different recombinant cCs including wild-type cC, amyloidogenic mutant cC I66Q, mutant cC I108T, and I108T/I66Q were examined by SDS-PAGE. PNGase F has been utilized extensively for demonstrating shifts in SDS-PAGE mobilities as an indication of *N*-glycosylation. As shown in Figure 1, after PNGase F treatment, the polysaccharide moiety was removed. The majority of the broad bands ~26 kDa of both recombinant mutant cC I108T and I66Q/I108T were reverted to the band at 14 kDa, similar to that of nonmodified cystatins, indicating that the release of polysaccharide generally results in a sufficient decrease in apparent molecular mass. It is noticeable that considerable amounts of glycosylated forms (the band at ~26 kDa) of cC mutant I108T and I108T/I66Q were secreted in addition to the nonglycosylated forms (the band at ~14 kDa), confirming that yeast *P. pastoris* can carry out glycosylation of the amide nitrogen of asparagines residues in a protein when found in

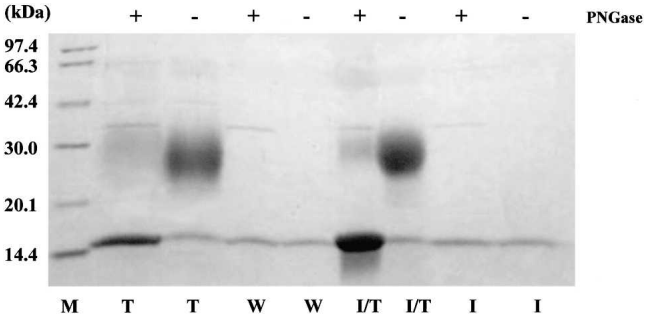

Figure 1. Mutant cC I108T and I66Q/I108T secreted as different forms by *P. pastoris* X-33. Samples of recombinant chicken cystatins (cC) and glycosylated cCs expressed from *P. pastoris* X-33 were treated with and without PNGase F before SDS-PAGE analysis. The glycosylated cC mutant I108T and I66Q/I108T were first denatured by 1× Glycoprotein Denaturing Buffer at 100°C for 10 min. Then 1/10 volume of each 10 ×G7 Buffer and 10% NP-40 were added. Finally, 1–5 μL PNGase F was added to the solution of denatured glycosylated cystatins and incubated at 37°C for 1 h. Lane *M*, molecular weight marker; lane *T*, mutant cC I108T; lane *W*, wild-type cC; lane *I*/*T*, mutant cC I108T/I66Q; lane *I*, amyloidogenic mutant cC I66Q. –, without PNGase F treatment; with PNGase F treatment. The gel sheet was stained with Coomassie brilliant blue.

the consensus sequence Asn-Xaa-Thr/Ser, providing *N*-linked glycosylation (Bretthauer and Castellino 1999). Generally in *P. pastoris*, a typical single *N*-linked oligosaccharide chain contains up to a dozen or so sugar residues, which is much shorter than those found in *Saccharomyces cerevisiae*. Nevertheless, with regard to our TOF-MS result (Fig. 5B, below) and the result of SDS-PAGE (Fig. 1), the molecular weights of the glycosylated forms of mutant cC I108T and I108T/I66Q were being calculated to range from 18,800 Da to 25,900 Da. The size of the polysaccharides was calculated to range from 30 to 60 mannose residues. In a previous research, Jiang and coworkers (Jiang et al. 2002; Tzeng and Jiang 2004) also examined the size of the polysaccharides attached on the same mutant cC I108T expressed in *P. pastoris* X-33 using phenyl-sulfuric acid reaction and the gel filtration chromatography method, a polymannosyl chain with 50° of polymerization per cystatin was deduced, which is in close agreement with our result.

Insoluble aggregate was hardly detected in cC mutant I108T/I66Q compared with that in amyloidogenic mutant cC I66Q

After cultivation of the transformants of recombinant cCs, the large amount of insoluble aggregate in the culture medium of amyloidogenic cC I66Q was collected by centrifugation at 11,900*g* for 30 min (Fig. 2A), while very little insoluble aggregate was detected in the culture medium of mutant cC I108T/I66Q. In contrast, such an insoluble aggregate was hardly found in the culture medium of the transformants of wild-type cC and the mutant cC I108T (Fig. 2B). All of the remaining supernatants were subjected to ammonium sulfate precipitation right after collection of the precipitates. The protein fraction precipitating between 10% and 40% saturation comprised mainly the polymeric form of recombinant cC, while the fraction precipitating between 50% and 60% saturation comprised the monomeric form (He et al. 2005a). On the basis of these results, the fractions precipitated with 10%–40%, 40%–50%, and 60% saturation were collected and then subjected to SDS-PAGE to determine the content of each fraction. The result in Figure 2B suggested that although the amyloidogenic cC muant I66Q was remarkably less soluble than that of the wild-type cC, the carbohydrate chains constructed on amyloidogenic cC mutant I66Q greatly improved the solubility of the broth of amyloidogenic cystatins.

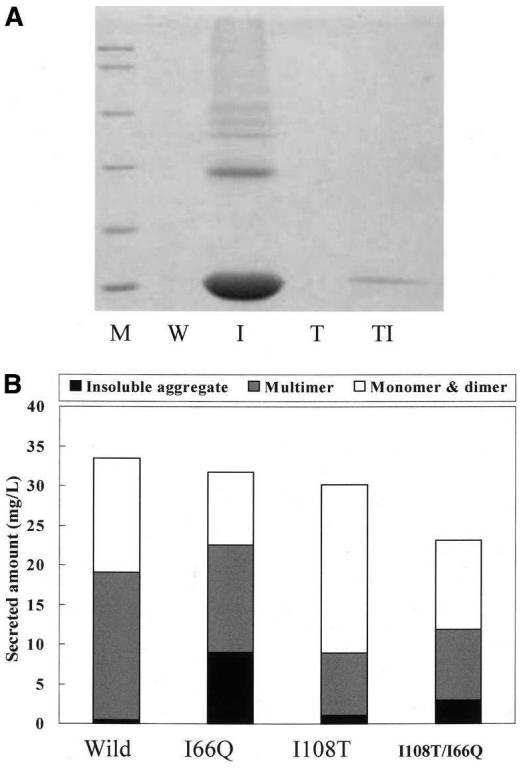

Figure 2. (*A*)SDS-PAGE analysis of insoluble aggregates detected in different recombinant cystatin cultures. After cultivation of the transformants of recombinant cCs, the insoluble aggregate in the culture medium was collected by centrifugation at 11,900*g* for 30 min. Lane *M*, molecular weight marker; lane *W*, wild-type cC; lane *I*, amyloidogenic mutant I66Q; lane *T*, cC mutant I108T; lane *I*/*T*, cC mutant I108T/I66Q. The gel sheets were stained with Coomassie brilliant blue. (*B*) Quantitative determination of the composition of the secreted protein amounts of different cystatins.

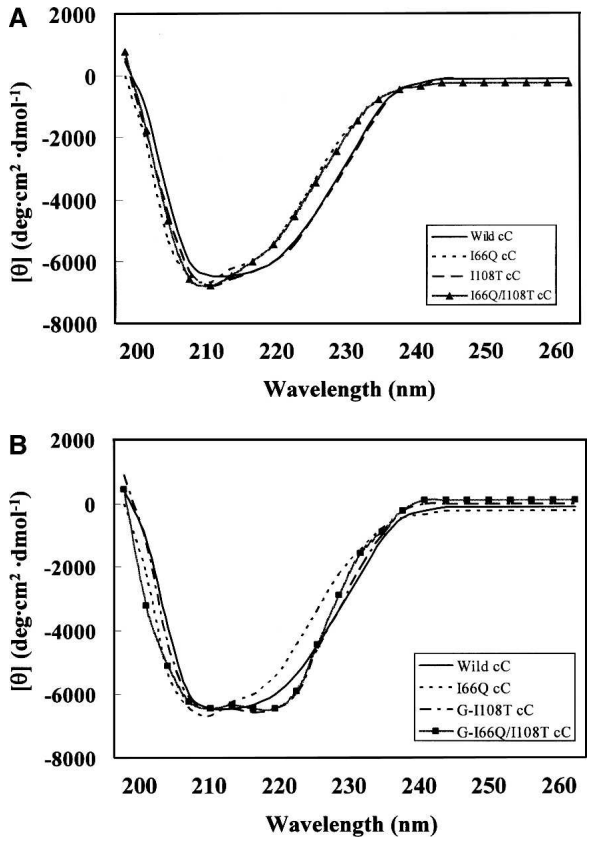

Figure 3. Far-ultraviolet-CD spectra of the wild-type cC, amyloidogenic mutant cC I66Q as well as both nonglycosylated forms (*A*) and glycosylated forms of mutant cC I108T and I66Q/I108T (*B*). The spectra were recorded at 25 °C and pH 7.0 on a J-600 spectropolarimeter.

Effect of glycosylation on the conformation of recombinant chicken cystatins

The secondary structures of glycosylated and nonglycosylated cystatins were all analyzed by far-UV circular dichroism (CD) spectroscopy. As shown in Figure 3A, the absolute minimum for both amyloidogenic mutant cC I66Q and nonglycosylated mutant cC I66Q/I108T showed a blue shift of the minimal value of CD spectra from 212 nm to 208 nm, indicating a certain level of change in β-structure. Interestingly, although the CD spectrum of nonglycosylated cC I108T closely coincided with that of wild-type cC, this mutant also showed a slight blue shift compared with that of wild-type cC, suggesting the unfolding tendency of the protein structure. On the contrary, both the glycosylated form of mutant cC I108T and the glycosylated form of mutant cC I66Q/I108T showed no substantial β-structure changes in CD spectra compared with that of wild-type cC (Fig. 3B). Since the depth in 222 nm of CD reflected the content of the α-helix, the slight increase in the absorbance at 222 nm of the glycosylated form of the cC mutant I66Q/I108T suggested the increased content of the α-helix, indicating that the polyglycosyl chain attached on Asn 106 inhibited the conformational changes caused by the replacement of the core hydrophobic residue at site 66.

Both glycosylated mutant cC I108T and glycosylated amloidogenic mutant cC I66Q/I108T exhibited enhanced inhibitory activity toward papain compared with nonglycosylated forms of cystatins

To further examine whether or not the introduced carbohydrate chains had significantly altered the tertiary structure of the cystatin mutants, the purified proteins were subjected to inhibitory activity analysis against papain. The equilibrium dissociation constants (K_i) of the complexes with papain were determined by inhibition under steady-state conditions (Table 1). Similar to wild-type and I66Q mutant recombinant cystatins, both the nonglycosylated mutant cC I108T and I66Q/I108T showed efficient but slightly reduced inhibitory activity toward papain (K_i being 3.4×10^{-12} M and 3.7×10^{-12} M, respectively). Whereas in the case of the glycosylated mutant cC I108T and I66Q/I108T, significant inhibition was observed, K_i being 2.6×10^{-12} M and 2.9×10^{-12} M, respectively, indicating a very strong binding relationship between the glycosylated proteins and papain.

The inhibitory activity toward papain was also detected on a substrate SDS-PAGE assay. The secreted protein samples of wild-type cC, mutant cC I66Q, as well as cC I108T and I108T/I66Q, were applied, as shown in Figure 4, A and B. While the monomeric forms of all of the nonglycosylated forms of recombinant cCs remained active, the two glycosylated forms of cCs exhibited increased inhibitory activity toward papain.

Glycosylation of recombinant cCs prevent the formation of dimers

To determine dimerization capacity of different recombinant cCs, the purified glycosylated amyloidogenic mutant cC I66Q/I108T and amyloidogenic cC I66Q were

Table 1. *Equilibrium constants for dissociation (K_i) of the complexes between papain and the different recombinant cystatins*

Inhibitor	K_i (pM)	±SD (pM)	*n*
Wild cC	2.5	±0.066	5
I66Q cC	2.7	±0.032	5
Nonglycosylated I108T cC	3.4	±0.047	6
Nonglycosylated I66Q/I108T cC	3.7	±0.059	5
Glycosylated I108T cC	2.6	±0.023	6
Glycosylated I66Q/I108T	2.9	±0.051	6

The standard deviation (SD) and number of measurements (*n*) used to calculate the mean K_i values given are indicated.

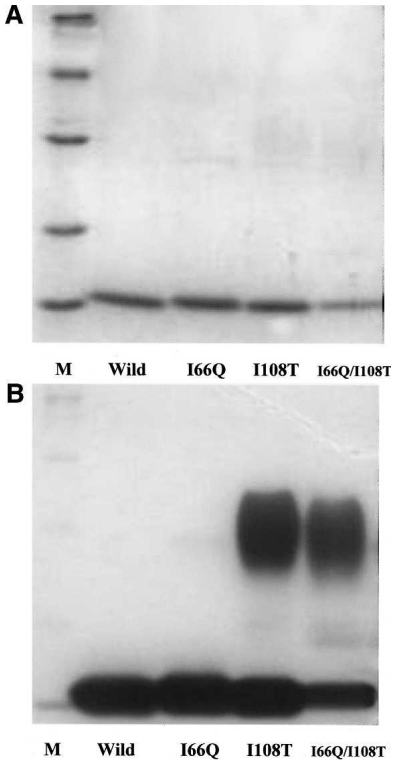

Figure 4. SDS-PAGE (*A*) and substrate SDS-PAGE (activity staining toward papain) (*B*) of the recombinant cCs expressed in *P. pastoris*. Lane *M*, molecular weight markers; lane *Wild*, wild-type cC; lane *I66Q*, amyloidogenic mutant cC I66Q; lane *I108T*, mutant cC I108T; lane *I66Q/I108T*, mutant cC I66Q/I108T. A 15% polyacrylamide gel containing 0.1% w/v casein was used for the activity assay; 0.5 μg of a sample protein was applied to each well of the gels. The bands of unhydrolyzed casein (Coomassie brilliant blue-stained) indicate the existence of cystatin. Both SDS-PAGE and substrate SDS-PAGE gel sheets were stained with Coomassie brilliant blue.

stored at 37°C in 20 mM phosphate buffer, pH 7.4 for 48 h, since the amyloidogenic variant L68Q of human cystatin C and the I66Q mutant of chicken cystatin had been shown to undergo dimerization and oligomerization under physiological conditions (37°C at pH 7.4) (Staniforth et al. 2001). Analysis of the composition of the resulting amyloidogenic cC I66Q sample by mass spectroscopy revealed the presence of dimers (Fig. 5A). Generally, the noncovalently bound dimers disassociated during MALDI-TOF mass spectroscopy; however, dimerization by domain swapping differs from other dimerization reactions by having a very high kinetic barrier. The high stability of the cC domain-swapped dimer, the formation of which is irreversible under accessible experimental conditions, contrasts the general case where the difference in the free energy between monomers and domain-swapped dimers is small (Staniforth et al. 2001). In the case of human cystatin C, a dimer is formed through β-sheet interactions, leading to the creation of an unusually long contiguous anti-parallel β-sheet formed by two copies of strands 2 and 3, which cross from one domain to the other with as many as 34 hydrogen bonds between the main chains and extra hydrogen bonds involving side chains. Once the dimer is formed, the L68Q human cystatin C dimer would be sufficiently stable (Janowski et al. 2004). Thus, dimerization through 3D domain swapping might be a distinct mechanism leading to the presence of the dimer peak.

In contrast to amyloidogenic cC I66Q, no dimers were detected for glycosylated cC mutant I66Q/I108T protein samples (Fig. 5B). Likewise, further TOF-MS analysis results of prolonged incubation samples also suggested that glycosylated cC mutant I66Q/I108T was resistant toward the formation of dimers. Since higher aggregates and the formation of cystatin C amyloid fibrils may arise through the 3D domain-swapping mechanism occurring in dimer formation (Janowski et al. 2001; Jaskolski 2001), it seems possible that inhibition of the formation of a domain-swapped dimer could also suppress the entire process of fibrillogenesis.

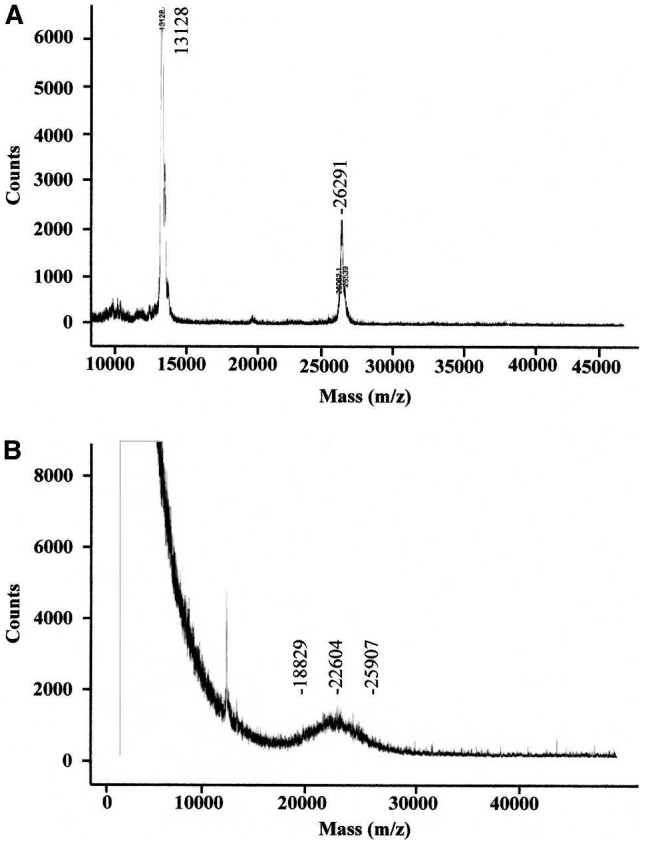

Figure 5. TOF-MS analysis of glycosylated mutant cC I66Q/I108T and amyloidogenic mutant cC I66Q after incubated at 37°C in 20 mM phosphate buffer (pH 7.4) for 48 h.

Fibril formation could be inhibited by glycosylation of the cystatins

To investigate whether or not typical amyloid fibril production from the amyloidogenic cC mutant I66Q could be suppressed by glycosylation, the fibrillogenicity of the glycosylated and nonglycosylated cC mutant I108T and I66Q/I108T were tested by thioflavin T fluorescence. Previously, several conditions for fibril formation were investigated, including different buffer (pH 2.0–7.0), different temperatures (37°C, 57°C), and the presence or absence of ethanol. Fibrils of wild-type cC were only found to be produced in solutions of low pH, and the production was accelerated by high temperature (Nilsson et al. 2004; Revesz et al. 2003) and ethanol addition (Goda et al. 2000). Our previous EM analysis for recombinant amyloidogenic mutant cC I66Q solutions incubated at 57°C in 100 mM hydrochloric acid–potassium chloride buffer, pH 2.0, containing 5% EtOH indicated the presence of fibrils (He et al. 2005a). As shown in Figure 6, after 12 d incubation of the I66Q cC sample under the same conditions, the relative Thioflavin T fluorescence value began increasing with the incubation time. Surprisingly, the fluorescence values of the nonglycosylated mutant cC I66Q/I108T and I108T also showed remarkable increases after 15 and 18 days of incubation, respectively (Fig. 6). In contrast, both the glycosylated mutant cC I66Q/I108T and the glycosylated mutant cC I108T did not show any change of the fluorescence value during the entire incubation period.

Moreover, EM studies were implemented to provide direct information about the fibril formation generated with different recombinant cystatins. As expected, the result of thioflavin T fluorescence kinetics is corroborated by the EM observation. Typical amyloid fibrils were clearly observed for cC I66Q and I108T after 35 d incubation, while nonglycosylated cC mutants I66Q/I108T showed virtually identical fibrils after 28 d incubation, which is even earlier than that of the amyloidogenic mutant cC I66Q (Fig. 7). On the other hand, no fibrils

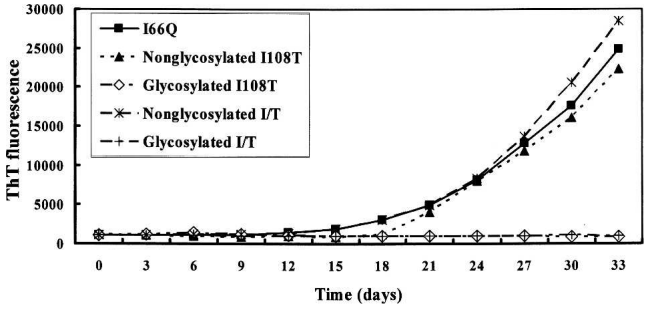

Figure 6. Kinetics of fibril growth measured by Thioflavin T fluorescence. Samples (1 μg/μL) were incubated at 57°C, in 66 mM glycine–hydrochloric acid buffer (pH 2.0), containing 5% EtOH.

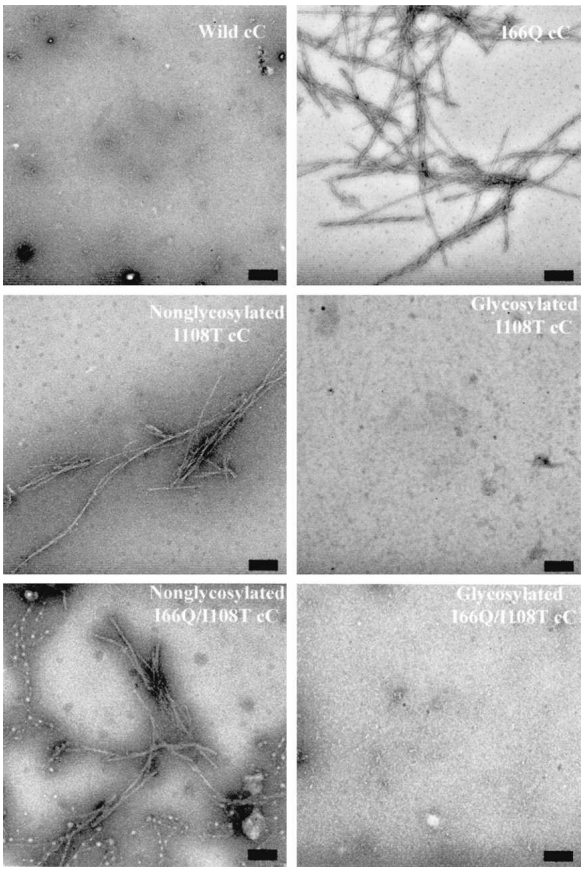

Figure 7. Electron microscopy of the wild-type cC, amyloidogenic mutant cC I66Q, glycosylated, and nonglycosylated mutant cC I108T and I66Q/I108T. Samples were incubated for 35 d at 57°C, in 66 mM glycine–hydrochloric acid buffer (pH 2.0), containing 5% EtOH. After incubation, suspensions of the samples were negatively stained and then examined by electron microscopy. (Bar = 200 nm.)

were observed for both of the two glycosylated forms of cystatins (Fig. 7). The width of the detected fibroid material was calculated to be in the range of 70–90 Å, which closely matches the widths of the fibers observed for many amyloidogenic proteins, including those of human cystatins (Staniforth et al. 2001).

All these data suggest the cystatin amyloid fibril formation could be inhibited by introduced *N*-glycosylation. Combined with the earlier finding in which this *N*-glycosylation prevented the formation of dimers, it seems possible that the introduced glycosylated chain might influence the exchange of the related domains of two cystatin fold units, thus further blocking the formation of amyloid fiber.

Discussion

The deposition of abnormal fibrillar protein aggregates has been observed in a wide range of tissues, and is now

associated not only with most of neurodegenerative diseases but also with a large number of other pathologies. The diseases caused by amyloid fibril includes bovine spongiform encephalopathy (BSE) and Creutzfeld-Jakob disease (CJD), and Alzheimer's disease, the fourth-highest cause of death in the developed world (Staniforth et al. 2001). It has now been established that wild-type hcC forms part of the amyloid deposits in brain arteries of elderly patients suffering from cerebral amyloid angiopathy (Grubb 2000). In hereditary cystatin C amyloid angiopathy (HCCAA), occurring endemically in the Icelandic population, a natural variant of HcC (Leu68Gln) forms massive amyloid deposits in brain arteries of young adults leading to lethal cerebral hemorrhage (Olafsson and Grubb 2000). Since in both cases aggregation involves abnormal, pathological change of protein conformation, these disorders can be classified as conformational diseases. Knowledge of the molecular pathophysiological mechanism causing the transition of physiologically normal and soluble proteins and peptides to toxic oligomers and insoluble fibrils is crucial in efforts to develop treatment modalities for this group of common diseases (Booth et al. 1997; Sipe and Cohen 2000; Jaskolski 2001; Ellis and Pinheiro 2002; Wetzel 2002; Dobson 2003).

The amyloid fibrils are irreversibly formed from a high-energy intermediate in equilibrium with an otherwise more stable monomeric protein in its native structure (Chen et al. 2002). In the case of the L68Q variant of human cystatin C, the mutation destabilized the folded state of the native human cystatin C structure, rendering the structural conversion from the folded state (native structure) to the transition state (high energy intermediate) more facile. The active monomeric mutants of both human cystatin C (L68Q) and chicken cystatin (I66Q) were known to dimerize under physiological conditions through 3D domain swapping (Staniforth et al. 2001). Our previous studies (He et al. 2005a), as well as the results in Figures 2 and 5A, had also demonstrated that the dimeric and oligomeric forms of I66Q cystatin were formed immediately after secretion. Moreover, the polymer can be further assembled from domain-swapped dimers via the interface between strands 1 and 5. Thus, large amount of insoluble forms of recombinant I66Q cC can be detected after expression.

Many reports had indicated that the introduction of *N*-glycosylation can facilitate the protein folding and subunit assembly, thus enhancing both the protein secretion amount and protein solubility (Nakamura et al. 1993, 1998). Therefore, we intend to employ both the wild-type cC and the amyloidogenic cC mutant I66Q as templates for the biosynthesis of novel glycoproteins and investigate the effect of glycosylation on protein expression and amyloid formation capability.

According to the well-studied crystal structure of hcC (Janowski et al. 2001) and the studies of Jiang et al. (2002), at positions 73, 78, and 106, which are not in the active site and exposed to the surface of chicken cystatin, the signal for *N*-linked glycosylation was created. Most importantly, we expected that the presence of the glycosylated chains at these positions would significantly destabilize the domain-swapped dimer relative to the glycosylated monomer because of the steric hindrance or interference introduced by the bulky carbohydrate chain. However, the desired *N*-glycosylation was found only in mutant cC I108T, leaving the general fold and the biological function of the protein unchanged.

The result in Figure 1 indicated that the carbohydrate chain had been covalently integrated into the potential *N*-glycosylation signal sequence in the carbonyl terminus of both wild and amyloidogenic chicken cystatins. As expected, the SDS-PAGE analysis result in Figure 2A suggested that the carbohydrate chains constructed on amyloidogenic cC mutant I66Q could improve the solubility of amyloidogenic cystatins.

Both of the glycosylated forms of mutant cC I108T and I66Q/I108T showed no substantial β-structure changes in CD spectra compared with that of wild-type cC, indicating that the glycosylation of proteins in yeast presents a positive relationship to the structural stability. The mutation site of I108T was located in close proximity to the hydrophobic core of cystatin, and it is known that the amino acid substitution of nonpolar hydrophobic isoleucine with polar hydrophilic glutamine at position 66 altered intrinsic properties leading to amyloidosis (Staniforth et al. 2001). The nonglycosylated mutant cC I66Q/I108T also showed an increased tendency of unfolding due to the replacement of isoleucine by polar hydrophilic amino acid threonine. Furthermore, the increase in the α-helix content and decrease in the β-structure strongly suggested that the carbohydrate chain greatly inhibited the structural change caused by amino acid substitution of isoleucine by glutamine and/or threonine.

On the other hand, it is also possible that the carbohydrate chain might give a hindrance to cystatin aggregation or fibrillization by playing the role of a cushion to prevent the collision of core proteins or other protein species (in this study, the glycosylated and nonglycosylated cystatins, respectively). TOF-MS analysis results showed that in contrast to amyloidogenic cC I66Q, no dimers were detected for glycosylated cC mutant I66Q/I108T protein samples after incubation under dimer formation conditions. Considering the carbohydrate chain was attached to the fifth β-strand of the cystatin molecue and the carbohydrates are large and hydrophilic, it is possible that the glycosylation could cause a steric effect that

inhibits the exchange of the two parts of monomeric cC which undergo swapping and the further connection of the β-sheets of the two cystatin-fold units via stand 1 and 5. Further thioflavin T fluorescence kinetics and EM studies also confirmed the higher stability of glycosylated forms of cystatins and their higher resistance to dimerization, oligomerization, and fibrillization, whereas all of the nonglycosylated cystatins except for wild-type cC showed fibrillogenicity under the same incubation conditions.

That the glycosylated mutant cC I66Q/I108T maintained virtually identical secondary structure to wild-type cC and that the glycosylation of the amyloidogenic cC inhibited fibrilization capacity of the protein are noteworthy when put in the context of our previous study (He et al. 2005b). In that study, our results on Eps1p, a novel membrane-bound chaperone in ER quality control, had demonstrated that wild-type cC secreted at a much higher level in Δ*eps1* yeast cells than that in wild-type yeast. In addition, the majority of the reports also showed that unbalanced chaperone amounts and chaperone capacity in aged organisms helps the accumulation of aggregated proteins, which often cause folding disease, mostly of the nervous system (Soti and Csermely 2003; Li et al. 2004). These observations, combined with the fact that the glycosylated proteins have different folding pathways in ER and require more chaperones to fold correctly than nonglycosylated proteins (Ellgaard et al. 1999), lead to the supposition that the pathophysiological mechanism of cerebral amyloid angiopathy suffered by elderly patients could possibly be explained by the formation of amyloid deposits by wild-type hcC in the brain arteries of elderly patients due to decreased levels of aging-related ER chaperones. This proposal provides insight into the possible treatment strategies based upon the regulation of the balance between chaperone requirement and availability.

Materials and methods

Materials

Restriction endonuclease, T4 DNA ligase, Pyrobest DNA polymerase, a DNA sequencing kit, and an mRNA selective PCR kit were purchased from Takara Shuzo. An RNeasy mini kit was purchased from Qiagen K.K. The pT7 Blue T-vector was from Novagen Merck. A QuikChange site-directed mutagenesis kit was purchased from Stratagene. Synthetic oligonucleotides were purchased from Kurabo. DNA sequencing was performed with a Thermo Sequenase Core sequencing kit from Amersham Japan. The Easy Select *Pichia* expression kit was purchased from Invitrogen Corp. Peptide–*N*-glycosidase F (PNGase F) was purchased from New England Biolabs. CM-Toyopearl resin was a product of Toso. Sephadex G-75 Superfine resin was purchased from Pharmacia. All other chemicals were of analytical grade for biochemical use.

Bacterial strains and plasmids

Escherichia coli XL-1 blue [*lac* (F′ proAB, lacI^{q}ZΔM15, Tn10 (Tet^R)) *rec*A1, *end*A1, *gyr*A96, *thi*-1, *hsd*R17, *sup*E44, *rel*A1], and Top10F′ (F′[*pro*AB, *lac*I^q, *lac*ZΔM15, Tn10(Tet^R)] *mcr*A, Δ (*mrrhsd*RMS-*mcr*BC), 80*lac*ZΔM15, Δ*lac*X74, *deo*R, *rec*A1, λ*ara*D139, Δ(*ara-leu*) 7697, *gal*U, *gal*K, *rps*L (Str^R), *end*A1, *nup*G), supplied by Amersham, were used as host cells in cloning experiments. *P. pastoris* X-33 (wild type, mut+) and the pPICZαA expression plasmid vector were purchased from Invitrogen.

Construction of cystatin expression vectors

Total RNA was isolated from chicken oviduct using an RNeasy mini kit. A DNA fragment encoding chicken cystatin was prepared from total mRNA by two-step RT-PCR using an mRNA-selective PCR kit. For insertion of the cystatin cDNA into the *P. pastoris* expression vector, the cystatin cDNA containing XhoI and XbaI sites was first cloned into subcloning vector pT7 blue T-vector, and then the cystatin cDNA was ligated with pPICZαA, an expression vector containing an *AOX1* promoter that allows methanol-inducible and high-level expression in yeasts. Finally, the SacI linearized DNA was transformed in *P. pastoris* cells by electroporation.

Quick-change site-directed mutagenesis

Construction of mutant I66Q is described as in our previous paper (He et al. 2005a). The mutant cC I108T and I108T/I66Q for *N*-glycosylation in-frame cDNAs of both wild-type and amyloidogenic mutant I66Q were constructed according to the paper by Jiang et al. (2002) and slightly modified. The synthetic oligonucleotide primers for mutant I108T and I108T/I66Q were 5′-CCAAACTAAACTGCTGGAAAGCAA GTGC-3′ and 5′-GTTTAGTTTGGTTTAGCCAAGGAATA CTGT-3′ as sense and anti-sense primers, respectively.

Expression of recombinant cCs

After the pPICZαA/cC plasmid had been transformed into the *P. pastoris* X-33 expression host, the expression vector was integrated into the genomic DNA due to the existence of the AOX promoter sequence. The successfully transformed colonies were cultivated for 18 h in YPD medium (1% yeast extract, 2% peptone, and 2% glucose). Subsequently, the cells were harvested by centrifugation (1500*g*, 5 min) and the cell pellets were suspended in 200 mL YPM medium (1% yeast extract, 2% peptone, and 0.5% methanol). To induce expression of the recombinant cCs, these cultures were incubated for 3 d at 30°C with shaking, with 100% methanol added every 24 h to obtain a final concentration of 0.5% methanol.

Purification of recombinant cCs

The cultivation media were first centrifuged at 3000*g* for 10 min to remove the cells. The supernatant was centrifuged at 11,900*g* for 40 min to collect the insoluble protein aggregates, and then the supernatant was fractionated with various ammonium sulfate concentrations to separate the monomer, dimer,

and polymer forms of cystatin. The proteins precipitated upon the addition of various concentrations of ammonium sulfate were collected by centrifugation at 11,900*g* for 40 min, and the precipitate was dissolved in 5 mL of phosphate buffer (50 mM at pH 7.0). The resultant solution was desalted by dialysis against phosphate buffer (50 mM at pH 7.0) overnight. The samples dissolved from the precipitation step were diluted and applied on a CM-Toyopearl column. The absorbed recombinant cCs were eluted in a gradient manner using 0–0.5 M sodium chloride in 20 mM Tris-HCl buffer (pH 7.5). The protein content of each fraction was determined by measuring the absorbance at 280 nm. The fraction containing the protein was collected and dialyzed against deionized water to remove salt at 4°C. To further purify the glycosylated forms of recombinant cCs, the solution was applied to a Sephadex G-75 superfine column (3 cm × 100 cm) equilibrated with 20 mM Tris-HCl buffer (pH 7.5) comprising 0.2 M sodium chloride, 0.01% BRIJ^{-}35 and 0.02% sodium azide. Finally, the protein content of each fraction was determined by measuring the absorbance at 280 nm. After precipitation of samples with different concentrations of ammonium sulfate was completed, the precipitates were dissolved and subjected to SDS-PAGE analysis.

Deglycosylation

The glycosylated cC mutants I108T and I66Q/I108T were first denatured by 1 × glycoprotein denaturing buffer at 100°C for 10 min. Then 1/10 volumes of each 10 × G7 Buffer and 10% NP-40 were added. Finally, 1–5 μL PNGase F was added to the solution of denatured glycosylated cystatins and incubated at 37°C for 1 h.

SDS-PAGE

SDS-PAGE was conducted according to the method of Laemmli (1970) using a 15% acrylamide separating gel and a 5% stacking gel containing 1% SDS. Samples were heated at 100°C for 5 min in Tris-glycine buffer (pH 6.8) containing 1% SDS and 1% 2-mercaptoethanol. Electrophoresis was carried out at a constant current of 10 mA for 5 h using an electrophoretic Tris-glycine buffer containing 0.1% SDS. The SDS-PAGE gel sheets were both stained with Commassie brilliant blue R-250.

TOF-MS

TOF-MS analysis was performed with a Voyager DE/PROJ (Perseptive Biosystems). The matrix, 3,5-dimethyl-4-hydroxciammic acid (sinapic acid), was dissolved in a reaction solution comprising equal volumes of acetonitrile and 0.1% TFA for recombinant chicken cystatins. The sample concentration was 1.5 mg/mL.

Circular dichroism (CD) analysis

The far-ultraviolet (200–260 nm) circular dichroism (far-UV CD) spectra were measured to estimate the conformational change in recombinant cystatins according to the method of Kato and Takagi (Kato et al. 1992). Recombinant cystatin solutions were adjusted to 0.01 mg/mL with distilled water. CD spectra were recorded at 25°C on a J-600 spectropolarimeter (Jasco) with a 1.0-cm cuvette.

Inhibitory activity

The methods used for active site titration and determination of equilibrium constants for the dissociation (K_i) of complexes between cystatin and papain have been described in detail (Fiedler et al. 1984). The cysteine protease inhibitory assay was performed using papain as the target enzyme and Z-Arg-Arg-NNap as its substrate with some modifications. The active concentrations of the wild-type and mutant cC I66Q were determined by titration with papain. The papain was previously active site-titrated using L-3-carboxy-2,3-*trans*-epoxypropionylleucylamido (4-guanidino)-butane (E64). The assay buffer was 73 mM sodium phosphate (pH 6.0), containing 2 mM cysteine and 1 mM EDTA to activate the enzyme. The absorbance of the cleaved 2-naphthylamine was measured at 520 nm with a Hitachi U-2000 spectrophotometer.

The inhibitory activity toward papain was also determined by substrate SDS-PAGE (Chen et al. 2001). Fifteen percent polyacrylamide gels containing 0.1% (w/v) casein were used for the activity assay; 0.5 μg of sample protein was applied to each well in the gels. After electrophoresis, the gels were prewashed with 2.5% Triton X-100 at least two times for 30 min to remove SDS, and then incubated in 0.10 M phosphate buffer containing 2 mM cysteine, 1 mM EDTA (pH 6.0), and papain (0.01 mg/mL) at 40°C for 150 min. Cystatin activity was abolished with the staining solution, 0.01% Coomassie brilliant blue, 40% methanol, and 10% acetic acid. Active cystatin zones were visualized as intense blue bands against a clear background on the gels after destaining with 25% ethanol and 10% acetic acid.

Thioflavin T fluorescence-derived kinetics

Thioflavin T fluorescence has been used to trace the kinetics of fibrillation (Le Vine 1999). Solutions of different protein samples (1 μg/μL) in 66 mM glycine–hydrochloric acid buffer (pH 2.0), containing 5% EtOH and 0.04% NaN_3 were incubated for 35 d. Samples of 20 μL were mixed with 80 μL of 2.5 mM thioflavin T solution in 10 mM potassium phosphate containing 150 mM NaCl (pH 7.0). Fluorescence intensities were measured at an excitation wavelength of 440 nm and an emission wavelength of 510 nm with a fluorescence spectrophotometer (Wallac 1420 ARVOsx, Perkin-Elmer).

Transmission electron microscopy

Samples of glycosylated and nonglycosylated different recombinant chicken cystatins (1.0 μg/μL) were incubated for 35 d at 57°C in 100 μL of 66 mM glycine–hydrochloric acid buffer (pH 2.0), containing 5% EtOH and 0.04% NaN_3. After incubation, the prepared samples were adsorbed on carbon-coated copper grids and negative stained with 2% phosphate tangustanic acid (pH 6.0). Micrographs were recorded at a nominal magnification of 1000 to 20,000 with an electron microscope (Hitachi, H-7600) operating at 80 kV.

Acknowledgments

We thank Shuhei Tanaka for expert assistance and access to electron microscopy, and Adam Gomez for revision of the manuscript.

References

Abrahamson, M. 1996. Molecular basis for amyloidosis related to hereditary brain hemorrhage. *Scand. J. Clin. Lab. Invest.* **56:** 47–56.

Abrahamson, M. and Grubb, A. 1994. Increased body temperature accelerates aggregation of the Leu-68 → Gln mutant cystatin C, the amyloid-forming protein in hereditary cystatin C amyloid angiopathy. *Proc. Natl. Acad. Sci.* **91:** 1416–1420.

Bode, W., Engh, R., Musil, D., Thiele, U., Huber, R., Karashikov, A., Brzin, J., Kos, J., and Turk, V. 1988. The 2.0 Å X-ray crystal structure of chicken egg white cystatin and its possible mode of interaction with cysteine proteinases. *EMBO J.* **7:** 2593–2599.

Booth, D.R., Sunde, M., Bellotti, V., Robinson, C.V., Hutchinson, W.L., Fraser, P.E., Hawkins, P.N., Dobson, C.M., Radford, S.E., Blake, C.C., et al. 1997. Instability, unfolding and aggregation of human lysozyme variants underlying amyloid fibrillogenesis. *Nature* **385:** 787–793.

Bosques, C.J. and Imperiali, B. 2003. The interplay of glycosylation and disulfide formation influences fibrillization in a prion protein fragment. *Proc. Natl. Acad. Sci.* **100:** 7593–7598.

Bretthauer, R.K. and Castellino, F.J. 1999. Glycosylation of *Pichia pastoris*-derived proteins. *Biotechnol. Appl. Biochem.* **30:** 193–200.

Chen, G.H., Tang, S.J., Chen, C.S., and Jiang, S.T. 2001. High-level production of recombinant chicken cystatin by *Pichia pastoris* and its application in mackerel surimi. *J. Agric. Food Chem.* **49:** 641–646.

Chen, P.Y., Lin, C.C., Chang, Y.T., Lin, S.C., and Chan, S.I. 2002. One O-linked sugar can affect the coil-to-β structural transition of the prion peptide. *Proc. Natl. Acad. Sci.* **99:** 12633–12638.

Dieckmann, T., Mitschang, L., Hofmann, M., Kos, J., Turk, V., Auerswald, E.A., Jaenicke, R., and Oschkinate, H. 1993. The structures of native chicken cystatin and of a recombinant unphosphorylate variant in solution. *J. Mol. Biol.* **234:** 1048–1059.

Dobson, C.M. 2003. Protein folding and misfolding. *Nature* **426:** 884–889.

Ekiel, I., Abrahamson, M., Fulton, D.B., Lindahl, P., Storerm, A.C., Levadoux, W., Lafrance, M., Labelle, S., Pomerleau, Y., Groleau, D., et al. 1997. NMR structural studies of human cystatin C dimers and monomers. *J. Mol. Biol.* **271:** 266–277.

Ellgaard, L., Molinari, M., and Helenius, A. 1999. Setting the standards: Quality control in the secretory pathway. *Science* **286:** 1882–1888.

Ellis, R.J. and Pinheiro, T.J. 2002. Medicine: Danger—Misfolding proteins. *Nature* **416:** 483–484.

Fiedler, F., Seemuller, U., and Fritz, H. 1984. Proteinases and their inhibitors. In *Methods of enzymatic analysis* (eds. J. Bergmeyer et al.), |vVol. 5, pp. 297–312. Verlag Chemie GmbH, Weinheim, Germany.

Goda, S., Takano, K., Yamagata, Y., Nagata, R., Akutsu, H., Maki, S., Namba, K., and Yutani, K. 2000. Amyloid protofilament formation of hen egg lysozyme in highly concentrated ethanol solution. *Protein Sci.* **9:** 369–375.

Gotte, G., Libonati, M., and Laurents, D.V. 2003. Glycosylation and specific deamidation of ribonuclease B affect the formation of three-dimensional domain-swapped oligomers. *J. Biol. Chem.* **278:** 46241–46251.

Grubb, A. 2000. Cystatin C—Properties and use as diagnostic marker. *Adv. Clin. Chem.* **35:** 63–99.

He, J., Song, Y., Ueyama N., Harada, A., Azakami, H., and Kato, A. 2005a. Characterization of recombinant amyloidogenic chicken cystatin mutant I66Q expressed in yeast. *J. Biochem.* **137:** 477–485.

He, J., Sakamoto, T., Song, Y., Saito, A., Harada, A., Azakami, H., and Kato, A. 2005b. Effect of *EPS1* gene deletion in *Saccharomyces cerevisiae* on the secretion of foreign proteins which have disulfide bridges. *FEBS Lett.* **579:** 2277–2283.

Janowski, R., Kozak, M., Jankowska, E., Grzonka, Z., Grubb, A., Abrahamson, M., and Jaskolski, M. 2001. Human cystatin C, an amyloidogenic protein, dimerizes through three-dimensional domain swapping. *Nat. Struct. Biol.* **8:** 316–320.

Janowski, R., Abrahamson, M., Grubb, A., and Jaskolski, M. 2004. Domain swapping in N-truncated human cystatin C. *J. Mol. Biol.* **341:** 151–160.

Jaskolski, M. 2001. 3D domain swapping, protein oligomerization, and amyloid formation. *Acta Biochim. Pol.* **48:** 807–827.

Jiang, S.T., Chen, G.H., Tang, S.J., and Chen, C.S. 2002. Effect of glycosylation modification (N-Q-(108)I → N-Q-(108)T) on the freezing stability of recombinant chicken Cystatin overexpressed in *Pichia pastoris* X-33. *J. Agric. Food Chem.* **50:** 5313–5317.

Kato, A., Kameyama, K., and Takagi, T. 1992. Molecular weight determination and compositional analysis of dextran-protein conjugates using low-angle laser light scattering technique combined with high-performance gel chromatography. *Biochim. Biophys. Acta.* **1159:** 22–28.

Laemmli, U.K. 1970. Cleavage of structural proteins during the assembly of the head of bacteriophage T4. *Nature* **227:** 680–685.

Le Vine, H. 1999. Quantification of β-sheet amyloid fibril structures with thioflavin T. *Methods Enzymol.* **309:** 274–284.

Lee, S. and Eisenberg, D. 2003. Seeded conversion of recombinant prion protein to a disulfide-bonded oligomer by a reduction-oxidation process. *Nat. Struct. Biol.* **10:** 725–730.

Li, D., Sun, F., and Wang, K. 2004. Protein profile of aging and its retardation by caloric restriction in neural retina. *Biochem. Biophys. Res. Commun.* **318:** 253–258.

Nakamura, S., Takasaki, H., Kobayashi, K., and Kato, A. 1993. Hyperglycosylation of hen egg white lysozyme in yeast. *J. Biol. Chem.* **268:** 12706–12712.

Nakamura, S., Ogawa, M., and Nakai, S. 1998. Effects of polymannosylation of recombinant cystatin C in yeast on its stability and activity. *J. Agric. Food Chem.* **46:** 2882–2887.

Nakamura, S., Hata, J., Kawamukai, M., Matsuda, H., Ogawa, M., Nakamura, K., Jing, H., Kitts, D.D., and Nakai, S. 2004. Enhanced anti-rotavirus action of human cystatin C by site-specific glycosylation in yeast. *Bioconjug. Chem.* **15:** 1289–1296.

Nilsson, M., Wang, X., Rodziewicz-Motowidlo, S., Janowski, R., Lindstrom, V., Onnerfjord, P., Westermark, G., Grzonka, Z., Jaskolski, M., and Grubb, A. 2004. Prevention of domain swapping inhibits dimerization and amyloid fibril formation of cystatin C: Use of engineered disulfide bridges, antibodies, and carboxymethylpapain to stabilize the monomeric form of cystatin C. *J. Biol. Chem.* **279:** 24236–24245.

Olafsson, I. and Grubb, A. 2000. Hereditary cystatin C amyloid angiopathy. *Amyloid* **7:** 70–79.

Revesz, T., Ghiso, J., Lashley, T., Plant, G., Rostagno, A., Frangione, B., and Holton, J.L. 2003. Cerebral amyloid angiopathies: A pathologic, biochemical, and genetic view. *J. Neuropathol. Exp. Neurol.* **62:** 885–898.

Sanders, A., Jeremy Craven, C., Higgins, L.D., Giannini, S., Conroy, M.J., Hounslow, A.M., Waltho, J.P., and Staniforth, R.A. 2004. Cystatin forms a tetramer through structural rearrangement of domain-swapped dimers prior to amyloidogenesis. *J. Mol. Biol.* **336:** 165–178.

Schwabe, C., Anastasi, A., Crow, H., McDonald, J.K., and Barrett, A. 1984. Cystatin: Amino acid sequence and possible secondary structure. *Biochem. J.* **217:** 813–817.

Sipe, J.D. and Cohen, A.S. 2000. Review: History of the amyloid fibril. *J. Struct. Biol.* **130:** 88–98.

Song, Y., Azakami, H., Hamasu, M., and Kato, A. 2001. In vivo glycosylation suppresses the aggregation of amyloidogenic hen egg white lysozymes expressed in yeast. *FEBS Lett.* **491:** 63–66.

Soti, C. and Csermely, P. 2003. Aging and molecular chaperones. *Exp. Gerontol.* **38:** 1037–1040.

Staniforth, R.A., Giannini, S., Higgins, L.D., Conroy, M.J., Hounslow, A.M., Jerala, R., Craven, C.J., and Waltho, J.P. 2001. Three-dimensional domain swapping in the folded and molten-globule states of cystatins, an amyloid-forming structural superfamily. *EMBO J.* **20:** 4774–4781.

Turk, V., Brzin, J., Longer, M., Ritonja, A., and Eropkin, M. 1983. Protein inhibitors of cysteine proteinases III. Amino acid sequence of cystatin from chicken egg white. *Hoppe-Seylers Z. Physiol. Chem.* **364:** 1487–1496.

Tzeng, S.S. and Jiang, S.T. 2004. Glycosylation modification improved the characteristics of recombinant chicken cystatin and its application on mackerel surimi. *J. Agric. Food Chem.* **52:** 3612–3616.

Wetzel, R. 2002. Ideas of order for amyloid fibril structure. *Structure (Camb.)* **10:** 1031–1036.